

# 3D simulation of accelerator conventional magnets with end pole defined by an analytical approach controlling multipoles and magnetic length

O.DELFERRIERE, D. DE MENEZES, R. DUPERRIER  
CEA, 91191 Gif-sur-Yvette, France

**Abstract** — During the design of a magnet, people generally pay particular attention to get the largest transverse section with small contribution of undesirable multipoles, and the 2D cross-section is adjusted in that way with a good accuracy. But the poles are often cut with sharp ends in the beam direction. Otherwise, in order to minimize the stray field to avoid interaction with other elements on the beam lines and corner saturation, it is common to define a simple 45° chamfer. The such truncated poles will create an amount of multipolar components that could exceed the magnet required tolerances. The magnetic length is also affected by the way that the truncation is done. We propose in this paper a handy analytical model that allows both to control integrated focusing forces and magnetic lengths for each type of conventional magnets (dipole, quadrupole, sextupole). The different end pole profiles are simulated with the 3D-program TOSCA for the dipole and the quadrupole cases. To estimate a possible damaging of optical qualities introduced by the end pole profile, we compare the multipolar components obtained by a 2D harmonic analysis at the magnet center, with an integrated one along the beam axis, taking into account the entire stray field. The results are then compared with those of the sharp end case.

## I. INTRODUCTION

During the past 10 years, the computer technology has made considerable progress and allows now to study complex electromagnetic problems with FEM based codes like TOSCA [1]. It is now possible to calculate accelerator magnets with a high accuracy (defects about a few  $10^{-5}$  in comparison with the ideal field). It is now absolutely necessary for some projects to reach such accuracy (SOLEIL [2]), where magnet tolerances required tends to a few  $10^{-4}$ . It is now possible to reach an accuracy that permit to suppress the shimming operation due to systematic multipolar components, during the magnetic measurements, by eliminating these components during the magnet definition.

Several attempts have been tested in order to get a consistent analytical model for designing chamfers. Langenbeck and Francsak have got good result for the control of undesirable multipoles [3]. But the obtained geometry of the chamfer was not easy and cheap to manufacture and a light coupling was introduced by used expansion. In the most of the cases, people use to proceed in several successive alterations. These alterations begin with a simple 45° chamfer and the profile is finally composed with a few slopes [4,5].

We propose in this paper to build electromagnets with pole tip profile that reduces considerably the amount of multipolar components with a method based on an analytical solution of Laplace equation. The geometry induced by this formula has also the advantage to be easy manufactured.

## II. ANALYTICAL MODEL AND SIMULATION TOOLS

### A. Analytical solutions of Laplace equation :

The most common state of art for tracking particles in magnetostatic channel is to use the following 2D serie to describe the magnetic field:

$$V(r, \theta) = \sum_n r^n (a_n \cos(n\theta) + b_n \sin(n\theta)) \text{ and } \vec{B} = -\vec{\nabla}V \quad \text{E. 1}$$

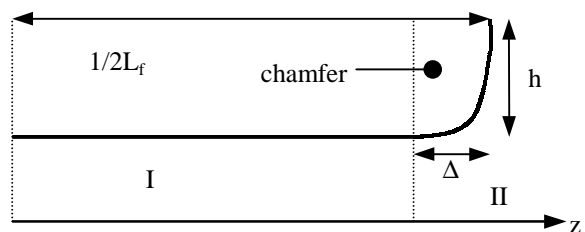


Fig. 1: Longitudinal profile from center to end of the magnet.

In practice, the magnets are not infinite, this induces  $z$  component. In order to get 3D representation of the field and a good continuity between the central region (I) and the end (II) of the magnet (Fig. 1), we propose the following serie [6,7]:

$$V(r, \theta, z) = (Az + B) \cdot \sum_n r^n (a_n \cos(n\theta) + b_n \sin(n\theta)) \quad \text{E. 2}$$

We make the assumption that magnet has a linear behavior and the discontinuity between regions for  $B_z$  can be neglected. Writing the previous expansion only for the desired multipole and setting magnetic length  $L_m$  equal to iron length  $L_f$ , we can obtain an analytical formula for the longitudinal profile of the chamfer:

$$r(z) = d \left( \frac{\Delta}{\frac{1}{2} L_f - z} \right)^{1/n} \quad \text{E. 3}$$

where  $n$  is the order of the multipole,  $d$  the minimum distance between the axis and the pole. This supposes that the multipolar content is poor in the central region (I). We will see that we can reach good performances.

### B. Simulation tools :

1) *Mesh generation* : The models have been built using the code for electromagnetic design, *Opera-3D* package [1] using finite element method.

Several implementations of this package have been developed at CEA/Saclay which allow us to get quickly models with smooth chamfers (Fig. 2). These chamfers are extrapolated from analytical formulas. Each multipole has its specific 3D profile (transverse+longitudinal).

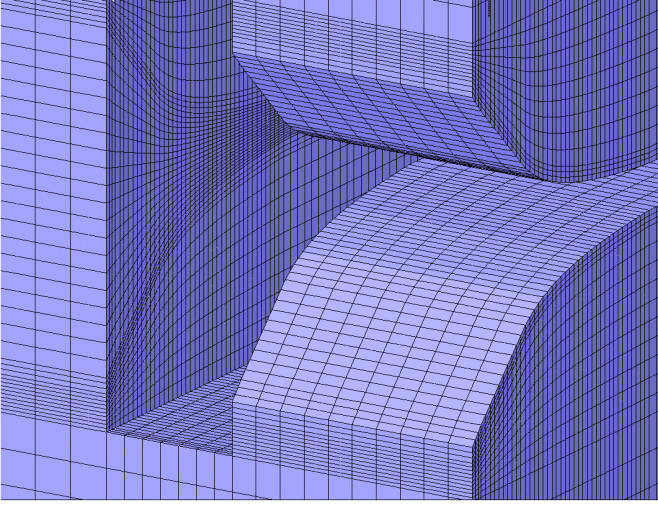


Fig. 2: Typical pole tip shape for the dipole

The model is submitted to the Opera-3D/Tosca solver which runs on a HP-J282 workstation, configured with 512 Mo of RAM. The CPU time necessary to solve the problem is about 15 hours for 15 non linear iterations depending on the number of finite elements in the model, but usually around 450 000 to ensure a very good accuracy.

2) *Post processing and harmonic analysis* : The multipolar tolerances given by the orbit calculations have to be reached taking into account the integral of these multipolar defaults along the whole particles trajectory in the magnet region, but in the stray field region too.

To estimate the influence of the stray field on the magnetic field multipolar analysis, we have calculated the surface integral of magnetic field components from  $-\infty$  to  $+\infty$  (in fact  $-L$  to  $+L$  where  $L$  is large enough), over a cylindrical surface of radius just below the value of half gap for the dipole, and bore radius for the quadrupole.

We start with the expression of the magnetic scalar potential  $V(r, \theta)$  in cylindrical coordinates :

$$V(r, \theta) = \sum_n \alpha_n r^n \sin(n\theta) \quad \text{E. 4}$$

By projection of  $V(r, \theta)$  on this expansion, we can get the  $\alpha_n$ :

$$\alpha_n = \frac{1}{\pi r^n} \int_0^{2\pi} V(r, \theta) \sin(n\theta) d\theta \quad \text{E. 5}$$

We define the “integrated harmonic term”  $A_n$  as:

$$A_n = \frac{1}{2\pi r^n L} \int_{-L}^{+L} \int_0^{2\pi} V(r, \theta, z) \sin(n\theta) d\theta dz \quad \text{E. 6}$$

where  $L$  is the integration length and  $z$  the beam axis. From the equation E.2, we can obtain the harmonic coefficients for magnetic field components  $B_r$  :

$$a_n = \frac{1}{\pi r^{n-1}} \int_0^{2\pi} B_r(r, \theta) \sin(n\theta) d\theta \neq 0 \quad \text{E. 7}$$

and the “integrated harmonic term”:

$$A'_n = \frac{1}{2\pi r^{n-1} L} \int_{-L}^{+L} \int_0^{2\pi} B_r(r, \theta, z) \sin(n\theta) d\theta dz \neq 0 \quad \text{E. 8}$$

To keep the agreement with orbit calculations, we have normalized all the 3D terms by the magnetic length defined by:

$$\frac{\int_{-L}^{+L} \int_0^{2\pi} B_r(r, \theta, z) \sin(p\theta) d\theta dz}{\int_0^{2\pi} B_r(r, \theta, 0) \sin(p\theta) d\theta} = L_m \quad \text{E. 9}$$

where  $p$  is fundamental harmonic ( $p=1$  for the dipole,  $p=2$  for the quadrupole, ...).

Automatic procedures have been written in Opera-3D language to calculate the surface integrals  $A'_n$  for  $n=1$  to  $n=20$  [8]. In the following sections, we will compare the harmonic analysis obtained on a magnet (dipole or quadrupole) with different pole tip shape characterized by its depth  $\Delta$  according to §II.A. . Theoretically,  $h$  is supposed to be infinite, but for building feasibility, at a certain height  $h_0 < h$ , the curvature of pole profile is going tangentially up to the magnet end face. All the simulations will be compared with the case of the magnet without any pole tip profile. The longitudinal profile of end shape is built with ten slopes.

### III. APPLICATION TO THE DIPOLE

#### A. Magnet description:

The dipole is a “C-shaped” one adapted from the design of the storage ring dipole of SOLEIL with simplifications for the easiness of building the model and varying its geometry. Its length is 1 meter long and it is not curved, instead of 1.052 meter and 5.36 meter radius. The air gap is 37 mm for a nominal induction of 1.56 T (Fig. 3). The lateral chamfers have been suppressed to simplify. The 3D model limited by symmetry and anti symmetry planes is restricted to one quarter of the dipole.

#### B. Pole tip shape :

We can derive from E.3 the equation of the longitudinal profile for the dipole in region II with  $g$  the half of the air-gap:

$$r(z) = g \frac{\Delta}{\frac{1}{2} L_f - z} \quad \text{E. 10}$$

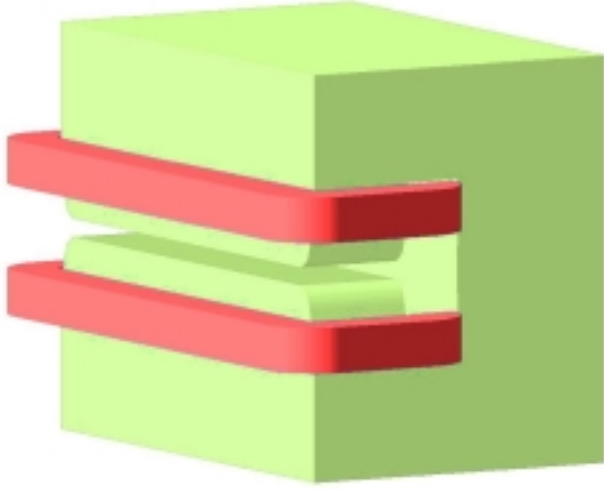


Fig 3: The entire dipolar magnet with conductors

The depth  $\Delta$  is function of the integral of the magnetic field required by beam dynamics  $B_{dyn} L_m$  (where  $L_m$  is the magnetic length and  $B_{dyn}$  is the constant value of magnetic field. We can write the expression of the depth  $\Delta$  as a function of  $B_{dyn}$ :

$$\Delta = L_f \left( 1 - \frac{B_{dyn} g}{\mu_0 NI} \right) \quad \text{E. 11}$$

For our study, we have increased  $\Delta$  in order to wander from the sharp end case. In some cases, we have taken into account the variation of the integral of the magnetic field by correcting the ampere-turns. If we have  $(NI)_1$  ampere-turns for a depth  $\Delta_1$  the ampere-turns  $(NI)_2$  corresponding to a depth  $\Delta_2$  is :

$$(NI)_2 = \frac{L_f - \Delta_1}{L_f - \Delta_2} (NI)_1 \quad \text{E. 12}$$

Following the procedure described in previous sections, we have computed the relative amplitude of each harmonic. The reference is the main harmonic. The Fig. 4 collects the different coefficients as a function of  $\Delta$ . It appears that more  $\Delta$  is long more the undesirable multipolar components can be

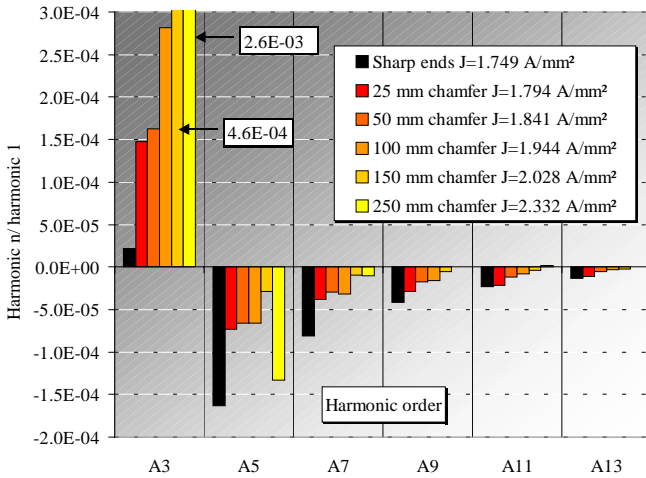


Fig. 4: Harmonics amplitude evolution as a function of  $\Delta$

reduced. But, increasing the current in order to keep constant the integral of  $B_r$ , the saturation rises in the truncated parts of the transverse section in such way that the sextupole (A3) rises. It's possible to cure this defect designing transverse chamfer. This phenomena implies an optimum for  $\Delta$  which depends on the initial level of saturation.

The figure 5 shows the harmonics amplitude evolution as a function of  $\Delta$  in the case where the integral is not compensated. For the two cases, the results don't depend significantly on  $h_0$ .

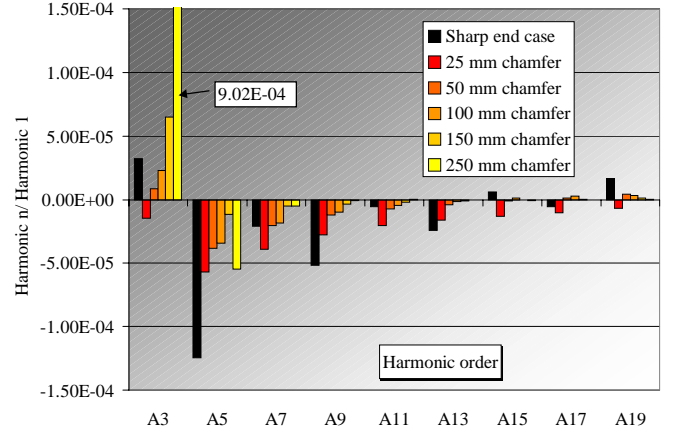


Fig. 5 : Harmonics amplitude evolution as a function of  $\Delta$

#### IV. APPLICATION TO THE QUADRUPOLE

##### A. Magnet description :

The quadrupole used for our study is another magnet of SOLEIL project for which a first pole tip shape study as been done by varying a simple 45° chamfer. It is the booster quadrupole, a symmetric one of 0.4 m long, with 57 mm bore radius, and a working gradient of 15.2 Tm<sup>-1</sup> (Fig. 6). Only one sixteenth of the magnet is modeled.

##### B. Pole tip shape :

Again, from E.3 the bore radius of the magnet function of the longitudinal position  $z$  can be extrapolated as:

$$r(z) = r_g \sqrt{\frac{\Delta}{\frac{1}{2}L_f - z}} \quad \text{E. 13}$$

where  $r_g$  is bore radius. The surface equation of the magnet in II is then:

$$xy - \frac{1}{2}(r(z))^2 = 0 \quad \text{E. 14}$$

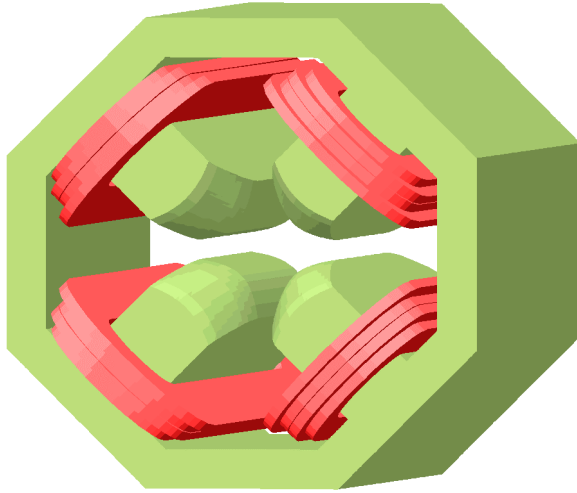


Fig. 6: The entire quadrupolar magnet with conductors

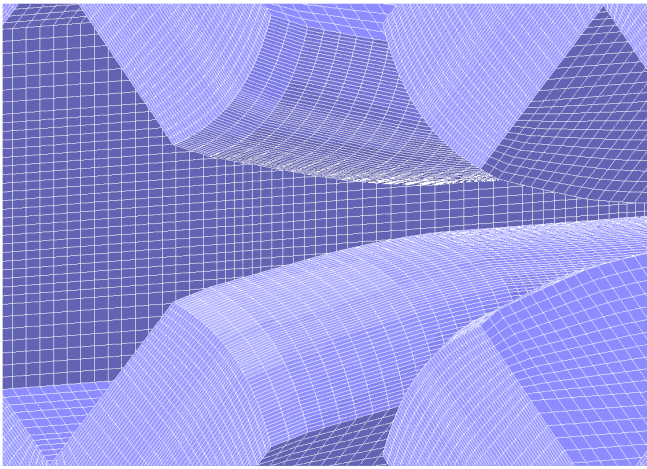


Fig 7: The geometry of the end pole around the axis.

We can observe that the hyperbolas are different for each  $z$ . The depth  $\Delta$  is equal to :

$$\Delta = L_f \left( 1 - \frac{G_{dyn} r_g^2}{2\mu_0 NI} \right) \quad \text{E. 15}$$

where  $G_{dyn}$  is the required nominal gradient.

If we want to work with constant integral value, we have also to correct the amperes-turns according to the same formula E.13. This procedure allows to determine the optimum for  $\Delta$  as for the dipole. In Fig.8, the relatives amplitudes of each harmonic are plotted for the case where the integral of the magnetic field is not compensated. We can remark the efficiency of the method. The amplitudes are divided by a factor 3.

We have checked that the results don't depend significantly on  $h_0$ . This proves that only the first slopes are important when the pole is close to the axis. The figure 7 shows the geometry of the quadrupole chamfer.

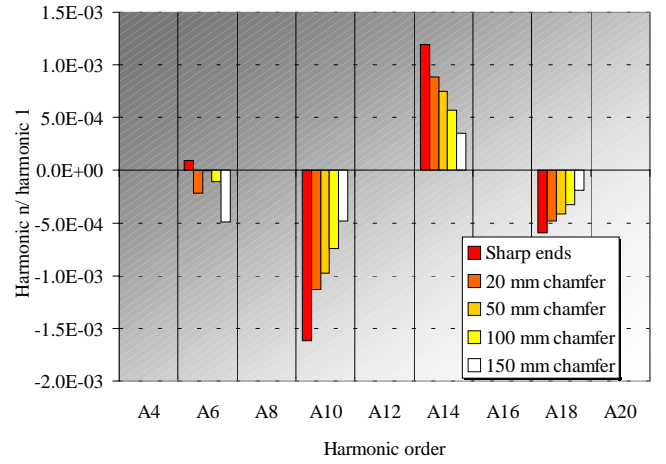


Fig. 8: Harmonics amplitude evolution as a function of  $\Delta$ .

## V. CONCLUSION

A consistent model based on a particular solution of Laplace equation has been built. Good performances have been achieved in undesirable multipoles cut. The expansion used remains very close of one used by orbit calculations. The method, tested here in the dipole and quadrupole cases, can be extended to any others multipoles. In the same time, we have shown that several slopes are necessary to build the end shape if good performances are needed. More, the first slope is not a classical  $45^\circ$  slope. The needed slopes depends on parameters like depth chamfer, the air-gap, the magnet total length and the main harmonic. Ten slopes were used in this study and seem to be a good compromise between the required smoothness and the feasibility of simulating and manufacturing the chamfer. Varying  $\Delta$ , the magnetic length can be adjusted.

We hope that the magnet designer will find in this work some attractive tools for building easily and accurately chamfers.

## REFERENCES

- [1] Opera-3D/Tosca, © Vector Fields Limited, Oxford, England
- [2] SOLEIL, Rapport d'Avant Projet Détaillé, CEA-CNRS, juin 1999
- [3] B. Langenbeck, B. Francsak, "Shaping of pole ends to minimize field errors in quadrupole magnets", IEEE Transaction on magnetics, Vol. 24, n°2, mars 1988
- [4] O. Delferrière, C. Evesque, J.P. Pénicaud, "Wide aperture conventional quadrupole for the  $t_{20}$  experiment at CEBAF", Proc. MT15, Vol. 1, 195 (1997)
- [5] M. Kumada, H. Sasaki, H. Someya and I. Sakai, "Optimization on the end-shaping of a quadrupole magnet", *Nuclear Instrument and Method* 211(1983) 283-286.
- [6] R. Duperrier, «Le potentiel électrique dans la zone utile d'un RFQ», internal report CEA/DSM/SEA/9844, (1998).
- [7] R. Duperrier, «A study of the R.F.Q. Radial Matching Section», internal report CEA/DSM/SEA/9967, (1999)..
- [8] O. Delferrière, "Décomposition harmonique sous OPERA-3D", internal report CEA/DSM/SEA/9923, (1999).